Eddy-current interaction with an ideal crack. II. The inverse problem

John R. Bowler
The University of Surrey, Guildford, Surrey GU2 5XH, United Kingdom

Stephen J. Norton
Oak Ridge National Laboratory, Oak Ridge, Tennessee 37830

David J. Harrison
Materials and Structures Department, Defence Research Agency, Farnborough, Hants. GU14 6TD, United Kingdom

(Received 30 September 1993; accepted for publication 16 February 1994)

Eddy-current inversion is the process whereby the geometry of a flaw in a metal is derived from electromagnetic probe measurements. An inversion scheme is described for finding the shape and size of cracks from eddy-current probe impedance measurements. The approach is based on an optimization scheme that seeks to minimize a global error function quantifying the difference between predicted and observed probe impedances. The error minimum is sought using a standard descent algorithm that requires a knowledge of the gradient of the error with respect to a variation of the flaw geometry. Computation of the gradient is based on a provisional flaw estimate, then the flaw estimate is updated in a "direction" that reduces the error. The process continues iteratively until a convergence criterion has been satisfied. Then the final flaw estimate should match the shape of the real defect. An equation for the gradient has been derived using an integral formulation of the ideal crack problem. Numerical estimates of the error gradient and the probe impedances have been calculated using approximations based on the moment method. Tests of the inversion scheme using single frequency probe impedance measurements have been carried out by calculating the shapes of narrow slots in aluminum alloy plates. Good agreement is found between the optimum profiles and the measured slot shapes.

I. INVERSION

In eddy-current nondestructive evaluation, a defect such as a crack in a metal is detected through changes of the probe signal caused by perturbations of induced current (Fig. 1). The task of predicting the signals from a knowledge of the probe and flaw is a direct or forward problem. In the corresponding inverse problem, the aim is to determine the shape and size of the flaw from probe signals measured at different positions and possibly at different frequencies. Time-domain measurements could also be used but the vast majority of eddy-current inspections are performed at a single frequency. Therefore, the primary interest is in the inversion of oscillatory signals.

An optimization approach to inversion seeks the flaw which minimizes the difference between tentative predictions of the probe signals and the measurements. If the agreement is unsatisfactory, then the flaw is updated and a new prediction made. The process continues through a number of iterations until predictions and observations match to within a reasonable tolerance. When a tolerable agreement has been found, the final flaw should be close to an optimum estimate of the real defect.

An improved estimate of the flaw is obtained if a global error quantifying the difference between predictions and the measurements is reduced. Generally it is not possible to reduce the error to zero owing to the effects of inaccuracies in the measurements or deficiencies in the predictions. However, a minimization search can be carried out using a descent algorithm that terminates once the error is below a predefined threshold. Because the inversion is inherently nonlinear, it is a possible that a false minimum is found in which case the final flaw estimate may be inaccurate. There are standard methods of dealing with local minima; for example, simulated annealing can be used to distinguish the global minimum, but they can be computationally expensive and are best avoided. Although the possibility of false minima cannot be discounted, they have not been encountered in the present investigation of ideal crack inversion.

In general, a flaw is represented by a flaw function defined in terms of a variation of the electrical properties of the material. There are a number of possible representations, two of which were explored in an earlier article.[1] For the first of these possibilities, the flaw function is defined as the electrical conductivity expressed as a function of position. A discrete version of this representation would be a piecewise constant approximation of the conductivity on a three-dimensional rectangular grid, which means that the inversion would seek the conductivity of each volume element in three dimensions. An unconstrained search for the conductivity of each cell is likely to be computationally expensive, therefore it would probably be necessary to limit the process in some way. The second possibility, leading to a more restricted optimization problem, arises for cases where it is known *a priori* that the defect is homogeneous; for example, if it is a cavity or a uniform inclusion. The inversion may then be specified as a search for the bounding surface.[1] Ideal crack inversion presents us with a third possible flaw function: the equation of the line following the crack edge. Here the aim is to devise a means of finding the shape of a crack in a known plane by calculating the position of the edge from a set of probe measurements.

With the above conception of the task, the search for the optimum crack shape takes place in a function space spanned

 0021-8979/94/75(12)/8138/7/$6.00

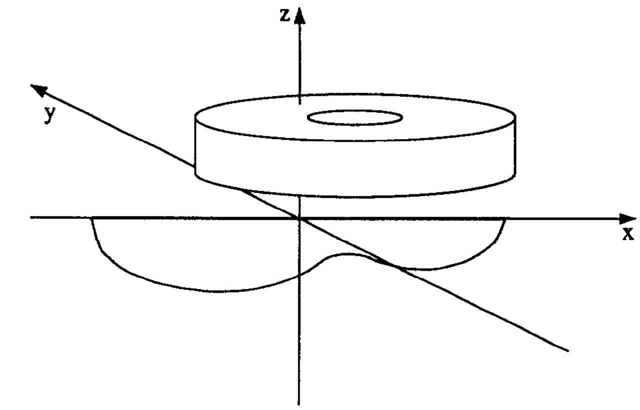

FIG. 1. A normal eddy-current coil over a surface breaking crack in an half-space conductor.

by all possible flaw functions in a particular class. In order to find the minimum error via a descent algorithm, it is necessary to determine the error gradient in this space with respect to a variation of the flaw. A knowledge of the gradient enables one to update the flaw in a "direction" that will guarantee an error reduction at each iteration. In crack inversion based on probe impedance measurements, the error gradient is dependent on the gradient of the impedance with respect to a variation in the location of the crack edge. Clearly the central requirement of the scheme is the determination of the impedance gradient.

In part I, the interaction of eddy currents with an ideal crack was calculated using a boundary integral method.[2] In the problem formulation, an integral equation for the field at the crack is derived, the equation is approximated using the moment method and a solution of the resulting linear system found by LU decomposition. This concluding part concerns the corresponding inverse problem. Previous work on crack inversion has been based on the thin skin limit where the skin depth is small compared with the depth of the crack.[3,4] In the present scheme, the skin depth is arbitrary. By developing the boundary integral theory further, an equation for the impedance gradient has been derived. Using this gradient and an extension of the numerical scheme for approximating the forward problem, inversions have been performed to find the shapes of simulated cracks from probe impedance measurements. Our account of ideal crack inversion begins with a brief review of the forward problem. Further details are given in part I.

II. FORWARD PROBLEM

An ideal crack is a perfect surface barrier to electrical current but has zero thickness. The current density on opposite sides of the surface will usually be different, therefore an ideal crack supports a discontinuity in the tangential electric field. A solution of the appropriate boundary-value problem may be found by representing the discontinuity by an equivalent source distribution that gives rise to the same field. A suitable source equivalent of an ideal crack in an electromagnetic field is a current dipole layer where the dipoles are orientated normal to the surface.[2]

The electric field perturbed by a crack at an open surface S_0 may be expressed as a surface integral using Green's second theorem. By applying a vector version of the theorem, it is found that the electric field in conductor containing an ideal crack is given by

$$\mathbf{E}(\mathbf{r})=\mathbf{E}^{(0)}(\mathbf{r})+i\omega\mu_0\int_{S_0}\mathscr{G}(\mathbf{r}|\mathbf{r}')\cdot\mathbf{p}(\mathbf{r}')dS', \tag{1}$$

where $\mathbf{E}^{(0)}(\mathbf{r})$ is the unperturbed electric field, $\mathbf{p}(\mathbf{r}')=\hat{n}p(\mathbf{r}')$ is the dipole distribution on the crack surface S_0, and $\hat{n}$ is a unit vector normal to the surface. The half-space dyadic Green's function, $\mathscr{G}(\mathbf{r}|\mathbf{r}')$, ensures that the solution satisfies the correct continuity and boundary conditions for a half-space conductor. Setting the normal component of the electric field to zero in the limit as the field point approaches the surface of the crack gives

$$E_n^{(0)}(\mathbf{r}_\pm)=-i\omega\mu_0\lim_{\mathbf{r}\to\mathbf{r}_\pm}\hat{n}\cdot\int_{S_0}\mathscr{G}(\mathbf{r}|\mathbf{r}')\cdot\mathbf{p}(\mathbf{r}')dS', \tag{2}$$

where $\mathbf{r}_\pm$ denotes the limit as the crack surface S_0 is approached from one side or the other. This equation for the dipole density will be written as

$$E_n^{(0)}(\mathbf{r}_\pm)=-i\omega\mu_0\int_{S_0}G^{nn}(\mathbf{r}_\pm|\mathbf{r}')p(\mathbf{r}')dS', \tag{3}$$

where $G^{nn}(\mathbf{r}|\mathbf{r}')=\hat{n}\cdot\mathscr{G}(\mathbf{r}|\mathbf{r}')\cdot\hat{n}$. Because of the nature of the singularity of the Green's function, the integral is to be interpreted using the Hadamard theory of the finite part.[5]

Equation (3) has been approximated using the moment method and the resulting linear system solved to give a piecewise constant estimate of the dipole density.[2] The probe impedance change due to an ideal crack is given by

$$Z=-\int_{S_0}E_n^{(0)}(\mathbf{r})p(\mathbf{r})dS \tag{4}$$

for unit probe current. A discrete approximation of Eq. (4) is used to predict the measurements.

III. NONLINEAR OPTIMIZATION

In ideal crack inversion the task is to find the boundary of the defect from a knowledge of the scattered field as acquired, for example, by measuring probe impedance as a function of position and frequency. It is assumed that the crack lies in a known plane but the shape and size are unknown and must be inferred from measurements. The crack geometry is represented by the equation of the line of the crack edge written as $\xi(s,t)=0$, where s and t are coordinates of a point in the crack plane. The probe impedance due to the flaw is a continuous function of position and the excitation frequency ω. These coordinates are combined in the vector $\mathbf{m}\equiv\{x,y,z,\omega\}$. The impedance is written as $Z[\xi,\mathbf{m}]$, where the square bracket containing ξ denotes a functional dependence on the flaw function.

A global "error" $\mathscr{E}[\xi]$ is defined by

$$\mathscr{E}[\xi]=\sum_i W(\mathbf{m}_i)|Z[\xi,\mathbf{m}_i]-Z_{\text{obs}}(\mathbf{m}_i)|^2, \tag{5}$$

where the summation is over all the observations and $Z_{\text{obs}}(\mathbf{m}_i)$ is the observed impedance at $\mathbf{m}_i$. The weighting function $W(\mathbf{m}_i)$ is used to give more or less weight to the data as necessary. The aim is to find the flaw function ξ that minimizes the global error.

Whether it is a steepest descent, a conjugate-gradient, or Levenberg–Marquardt scheme that is chosen, it is necessary to calculate the gradient of the error with respect to a variation of the flaw function. An incremental variation of the flaw function means that the location of the crack edge is changed by adding or subtracting a small strip of territory to the perimeter of the crack domain. Suppose a variation in the flaw function $\delta\xi(t)$ results in the addition to the crack domain of a strip $\delta s(t)$ wide, where t is a coordinate measured along the crack edge and s is measured in the orthogonal direction in the crack plane. Then

$$\delta\xi(t) = -\frac{\partial\xi}{\partial s}\,\delta s(t).$$

Without loss of generality, the flaw function will be scaled in order that $\partial\xi/\partial s = -1$ enabling us to equate $\delta\xi(t)$ with the width of the strip.

Adding the strip to the perimeter of the crack domain gives rise to a change in the global error. Each part of the strip contributes to the change and by integrating the contributions, the total error increment is expressed as

$$d\mathscr{E}[\xi,\delta\xi] = \int_{\text{edge}} \nabla_\xi \mathscr{E}(t)\,\delta\xi(t)\,dt. \tag{6}$$

This relationship introduces $\nabla_\xi\mathscr{E}(t)$, the functional gradient of the error with respect to a variation of the flaw function. It represents the change in the global error due to a variation of the crack boundary at t. In a similar way the impedance gradient may be defined such that a change of impedance due to an incremental but arbitrary flaw variation is given by

$$dZ[\xi,\delta\xi,\mathbf{m}] = \int_{\text{edge}} \nabla_\xi Z(\mathbf{m},t)\,\delta\xi(t)\,dt. \tag{7}$$

The impedance gradient $\nabla_\xi Z(\mathbf{m},t)$ may be viewed as sensitivity function since it represents the effect on the impedance at $\mathbf{m}$ due to a change in the location of the edge of the crack at a point whose coordinate is t.

Substituting Eq. (5) into the definition of the functional derivative,

$$\begin{aligned} d\mathscr{E}[\xi,\delta\xi] &\equiv \lim_{\beta\to 0} \frac{\mathscr{E}[\xi+\beta\delta\xi]-\mathscr{E}[\xi]}{\beta} \\ &= \frac{d}{d\beta}\mathscr{E}[\xi+\beta\delta\xi]\big|_{\beta=0}, \end{aligned} \tag{8}$$

and using Eq. (7) gives

$$\begin{aligned} d\mathscr{E}[\xi,\delta\xi] = \int_{\text{edge}} \Bigg(& 2\ \mathrm{Re} \sum_i \left[Z[\xi,\mathbf{m}_i]\right. \\ & \left. -Z_{\text{obs}}(\mathbf{m}_i)\right]^* \nabla_\xi Z(\mathbf{m}_i,t) \Bigg)\,\delta\xi(t)\,dt. \end{aligned} \tag{9}$$

Hence, comparing Eq. (6), one identifies

$$\nabla_\xi\mathscr{E}(t) = 2\ \mathrm{Re} \sum_i \left[Z[\xi,\mathbf{m}_i]-Z_{\text{obs}}(\mathbf{m}_i)\right]^* \nabla_\xi Z(\mathbf{m}_i,t). \tag{10}$$

Equation (10) enables one to calculate the error gradient from a knowledge of the impedance gradient at all the observation points.

In order to find the optimum flaw function, the error gradient is evaluated and the boundary of the flaw updated using a formula that depends on the descent algorithm. Let the modified flaw function be $\xi+\Delta\xi$, then the steepest descent update is given by

$$\Delta\xi(t) = -\alpha\nabla_\xi\mathscr{E}(t), \tag{11}$$

where α governs the step size and is chosen to minimize the error functional $\mathscr{E}[\xi]$ in the direction of the gradient. Iteration continues until the condition $\mathscr{E}[\xi]<\epsilon$ has been satisfied, where ϵ is a real positive constant representing a tolerable residual error. Alternatively the process is terminated when the error no longer decreases significantly.

Evaluation of the error gradient from Eq. (10) requires first the impedance predictions $Z[\xi,\mathbf{m}_i]$, for all i and second the impedance gradient $\nabla_\xi Z(\mathbf{m}_i,t)$. The predictions are found from the solution of multiple forward problems. Assuming a suitable solver is available, the optimization problem reduces to one of finding the impedance gradient. A possible way forward is to approximate the impedance gradient as a discrete form at this point, replacing it with a sensitivity matrix. The matrix elements could be evaluated using a finite difference scheme but the use of finite differences for this purpose has potentially a very high computational cost that is best avoided. A more elegant approach is to postpone the discretization and extend the field theory with the aim of expressing the functional gradients in terms of the electromagnetic field at the flaw.

In an earlier article it was shown that the impedance gradient can be found in general from the same solutions that are used in predicting the impedances, plus an equal number of solutions from the corresponding adjoint problems.[1] These adjoint problems are defined in terms of an operator acting on the dipole density, as in Eq. (2), where an integral form for the operator is employed. If the operator is self-adjoint, the expressions for the impedance gradient simplify a little, but more significantly the computational effort needed to calculate it is halved because the adjoint problems are identical to the regular problems. Below we treat a special case of the ideal crack in which the surface of the crack is perpendicular to the surface of a half-space conductor. For this and similar calculations, each standard forward problem and its adjoint are the same. This means that an inversion from N measurements requires the solution of only N rather than $2N$ forward problems to give both the predictions and the impedance gradient at each iteration. If the crack were inclined to the air-conductor interface, the operator would not be self-adjoint and it would be necessary to solve two forward problems for each measurement.

IV. IMPEDANCE VARIATION

Consider an ideal crack in the plane $x=0$ perpendicular to the surface of a half-space conductor occupying the region $z<0$. A variation of the flaw will be defined in terms of a flaw characteristic function $\gamma(\mathbf{r})$ where

$$\gamma(\mathbf{r})=\begin{cases}1, & \mathbf{r}\in S_0,\\ 0 & \text{otherwise.}\end{cases} \tag{12}$$

The impedance variation resulting from an arbitrary incremental change in the flaw characteristic is

$$dZ=-\int_{S_E} E_x^{(0)}(\mathbf{r})dp(\mathbf{r})dS. \tag{13}$$

Here and throughout this section the functional dependence on ξ is implied but not stated and $\mathbf{r}\in S_E$. We have chosen to integrate over an extended domain in the plane of the crack, denoted by S_E, rather than the crack region S_0. This is simply a device for making the region of integration flaw independent. The extended domain is larger than that of the flaw, either before or after variation, but it is otherwise arbitrary. By defining $p(\mathbf{r})$ and $dp(\mathbf{r})$ as nonzero over the flaw region and zero otherwise, the extension of the region of integration makes no difference to the integral. In order to identify the impedance gradient introduced in Eq. (7), Eq. (13) is transformed into a line integral whose path is the edge of the crack.

An equation for $dp(\mathbf{r})$ is found by considering the equivalent of Eq. (2) for the varied flaw, namely

$$\begin{aligned}E_x^{(0)}(\mathbf{r})[\gamma(\mathbf{r})+\delta\gamma(\mathbf{r})]\\ =-i\omega\mu_0[\gamma(\mathbf{r})+\delta\gamma(\mathbf{r})]\\ \times\int_{S_E} G^{xx}(\mathbf{r}|\mathbf{r}')[p(\mathbf{r}')+dp(\mathbf{r}')]dS',\end{aligned} \tag{14}$$

where $\delta\gamma(\mathbf{r})$ is unity in the region of the flaw variation, the strip region, and zero elsewhere. The presence of the flaw characteristic in this equation means that it is valid for any field point in the plane of the flaw. Take the normal component of Eq. (1), multiply it by $\gamma(\mathbf{r})+\delta\gamma(\mathbf{r})$, extend the range of integration, and subtract Eq. (14) to give

$$\begin{aligned}E_x(\mathbf{r})\delta\gamma(\mathbf{r})=-i\omega\mu_0[\gamma(\mathbf{r})+\delta\gamma(\mathbf{r})]\\ \times\int_{S_E} G^{xx}(\mathbf{r}|\mathbf{r}')dp(\mathbf{r}')dS'.\end{aligned} \tag{15}$$

Note that the total electric field normal to the unvaried crack is zero, therefore $E_x(\mathbf{r})\gamma(\mathbf{r})=0$. The left-hand side of Eq. (15) represents a component of the electric field at the crack tip, prior to the variation. At the tip, the field exhibits a characteristic edge singularity that is described more fully in the following. For immediate purposes, note that there are two distinct relationships to be drawn from Eq. (15). The first states that the normal component of the electric field at the strip prior to the crack variation, $E_x(\mathbf{r})\delta\gamma(\mathbf{r})$, is equal and opposite to the field in that region due to the variational change in the dipole density. This relationship, stated as

$$E_x(\mathbf{r})\delta\gamma(\mathbf{r})=-i\omega\mu_0\delta\gamma(\mathbf{r})\int_{S_E} G^{xx}(\mathbf{r}|\mathbf{r}')dp(\mathbf{r}')dS', \tag{16}$$

ensures the normal electric field at the strip surface of the varied crack is zero. The second relationship follows by restricting Eq. (15) to the original crack domain, giving

$$-i\omega\mu_0\gamma(\mathbf{r})\int_{S_E} G^{xx}(\mathbf{r}|\mathbf{r}')dp(\mathbf{r}')dS'=0, \tag{17}$$

which means that the normal electric field at the surface of the unvaried crack is unchanged, in fact remains zero, after the crack is varied. In other words the normal field due to $dp(\mathbf{r})$ is zero over the surface of the original crack.

Equation (13) is transformed by substituting for $E_x^{(0)}(\mathbf{r})$ from Eq. (14). This gives

$$\begin{aligned}dZ=-\int_P E_x^{(0)}(\mathbf{r})dp(\mathbf{r})dS=i\omega\mu_0\int_{S_E}[\gamma(\mathbf{r})+\delta\gamma(\mathbf{r})]\\ \times\int_{S_E} G^{xx}(\mathbf{r}|\mathbf{r}')[p(\mathbf{r}')+dp(\mathbf{r}')]dS'\ dp(\mathbf{r})dS.\end{aligned} \tag{18}$$

Reversing the order of integration and using Eq. (16) gives

$$\begin{aligned}dZ&=-\int_{S_E}[p(\mathbf{r}')+dp(\mathbf{r}')]E_x(\mathbf{r}')\delta\gamma(\mathbf{r}')dS'\\ &=-\int_{S_E} dp(\mathbf{r}')E_x(\mathbf{r}')\delta\gamma(\mathbf{r}')dS',\end{aligned} \tag{19}$$

where we have used the fact that $G^{xx}(\mathbf{r}|\mathbf{r}')=G^{xx}(\mathbf{r}'|\mathbf{r})$.

The symmetry property of the xx component of the dyadic Green's function means that the integral operator is self-adjoint in the sense considered here.[1] It is this property that makes the regular and adjoint forward problems identical. Indeed, the same is true for any crack whose surface is normal to the conductor-air interface. On the other hand, the excitation of z components of the dipole distribution on an inclined crack will bring into play components of the half-space dyad that do not exhibit the self-adjoint property.[2] Therefore, a calculation of the impedance gradient in such cases requires the solution of distinct adjoint problems.

Equation (19) can be cast in the form of Eq. (7) by integrating over the width of the strip. In order to do this integration explicitly, the variation of the dipole density at the edge of the crack and the field at the crack tip is needed.

V. LOCAL EDGE SOLUTION

In a region whose dimensions are small compared with a skin depth, the electric field can be approximated as the gradient of a scalar potential satisfying the Laplace equation. In such a region, close to a crack with a smooth edge, the curvature of the edge can be neglected and the field described adequately by a scalar potential of the form

$$V(\rho,\phi)=-\mathscr{F}\rho^{1/2}\cos\left(\frac{\phi}{2}\right), \tag{20}$$

where ϕ is measured from the positive crack face and ρ is a radial coordinate defined with respect to an axis along the

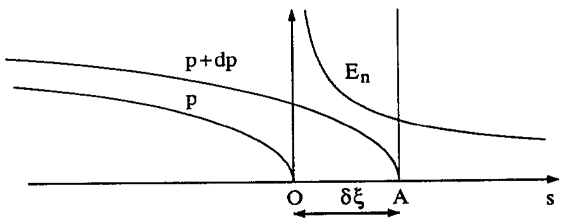

FIG. 2. Variation of the dipole density and the normal component of the electric field near the crack edge.

crack edge. The term $\mathscr{F}$ is locally constant and determines the overall strength of the edge field. The local electric field is given by

$$\mathbf{E}(\rho,\phi)=-\nabla V(\rho,\phi). \tag{21}$$

Using the general relationship between the dipole density and the jump in the electric field at the crack, Eq. (3) of part I, we find that the dipole density at the edge is given by

$$p(\rho)=2\mathscr{F}\sigma\rho^{1/2}, \tag{22}$$

where σ is the electrical conductivity of the conductor. The electric field in the vicinity of the crack tip is given by

$$\mathbf{E}(\rho,\phi)=-\nabla V=-\left\{\hat{\rho}\,\frac{\partial V}{\partial\rho}+\hat{\phi}\frac{1}{\rho}\frac{\partial V}{\partial\phi}\right\}$$
$$=\frac{\mathscr{F}}{2\rho^{1/2}}\left[\hat{\rho}\cos\left(\frac{\phi}{2}\right)-\hat{\phi}\sin\left(\frac{\phi}{2}\right)\right]. \tag{23}$$

The above local field is found in the limit as one approaches the edge of an arbitrary ideal crack having a smooth boundary. On the scale of the crack dimensions however, the term $\mathscr{F}$ will not be constant but vary along the edge. Therefore, for the general case, we define

$$\mathscr{F}(\mathbf{m},t)=\lim_{\rho\to 0}\rho^{1/2}[\mathbf{E}(\rho,\phi=0,t)-\mathbf{E}(\rho,\phi=2\pi,t)]\cdot\hat{\rho}, \tag{24}$$

where $\mathbf{E}(\rho,\phi=0,t)-\mathbf{E}(\rho,\phi=2\pi,t)$ is the jump in the electric field at the crack surface.

VI. IMPEDANCE GRADIENT

In evaluating Eq. (19) for an arbitrary ideal crack, the dipole density at the crack edge will be written, in accordance with the preceding discussions, as

$$\delta\gamma(s,t)dp(s,t)=2\sigma\mathscr{F}(\mathbf{m},t)\sqrt{\delta\xi(t)-s},\quad 0\leqslant s\leqslant\delta\xi, \tag{25}$$

where s is a coordinate in the crack plane measured outward in a direction normal to the edge of the unvaried crack (Fig. 2). At the edge of the varied crack, point A in Fig. 2, $s=\delta\xi(t)$. Equation (25) has the form of the local solution (22).

The singular electric field normal to the crack plane at the tip of the unvaried crack has the form given by the ϕ component of Eq. (23) with $\phi=\pi$. Thus,

$$E_x(s,t)=-\mathscr{F}(\mathbf{m},t)\,\frac{1}{2\sqrt{s}}. \tag{26}$$

Substituting Eqs. (25) and (26) into Eq. (19) and using the definition (8) gives

$$dZ[\xi,\delta\xi,\mathbf{m}]=\sigma\lim_{\beta\to 0}\frac{1}{\beta}\int_{\mathrm{edge}}\int_0^{\beta\delta\xi(t)}\mathscr{F}^2(\mathbf{m},t)$$
$$\times\left(\frac{\beta\delta\xi(t)-s}{s}\right)^{1/2}ds\,dt$$
$$=\frac{\pi\sigma}{2}\int_{\mathrm{edge}}\mathscr{F}^2(\mathbf{m},t)\,\delta\xi(t)dt, \tag{27}$$

which is the desired form for $dZ[\xi,\delta\xi,\mathbf{m}]$. Comparing with Eq. (7), one identifies

$$\nabla_\xi Z(\mathbf{m},t)=\frac{\pi\sigma}{2}\mathscr{F}^2(\mathbf{m},t). \tag{28}$$

This central result gives the impedance gradient in terms of a function $\mathscr{F}^2(\mathbf{m},t)$ which weights the dipole distribution at the edge of the crack.

The inversion algorithm begins by solving the forward problem for some initial estimate of the flaw shape. The solution is computed for each probe position giving a set of dipole distributions and impedance predictions. The dipole distribution at the edge of the crack is used to determine $\mathscr{F}^2(\mathbf{m},t)$ and the corresponding impedance gradient is calculated from Eq. (28). Next the error gradient is evaluated using Eq. (10) and the flaw is updated using the steepest descent formulas, Eq. (11). The process continues iteratively until a convergence condition is satisfied.

VII. NUMERICAL INVERSION

A number of tests of the inversion scheme have been carried out using experimental data obtained by measuring coil impedance due to interactions with simulated defects in metal plates. The skin depth was much smaller than the plate thickness for all observations, therefore no significant errors are introduced by treating the conductor as a half-space.

TABLE I. Probe and flaw parameters.

Coil parameters		
inner radius (a_1)	2.51±0.01 mm	
outer radius (a_2)	7.38±0.01 mm	
length ($2b$)	4.99±0.01 mm	
lift-off (l)	0.313±0.01 mm	
number of turns	4000	
Frequency	350 Hz	
Conductor		
conductivity	22.62±0.06 MS/m	
thickness	24 mm	
Flaw		
shape	semielliptical	irregular
length (d)	22.1±0.02 mm	49.78±0.05 mm
depth (h)	8.61±0.05 mm	8.94±0.05 mm
opening (c)	0.33±0.01 mm	0.33±0.01 mm
Derived quantities		
skin depth (δ)	5.65±0.02 mm	
opening/skin depth (c/δ)	0.058±0.002	

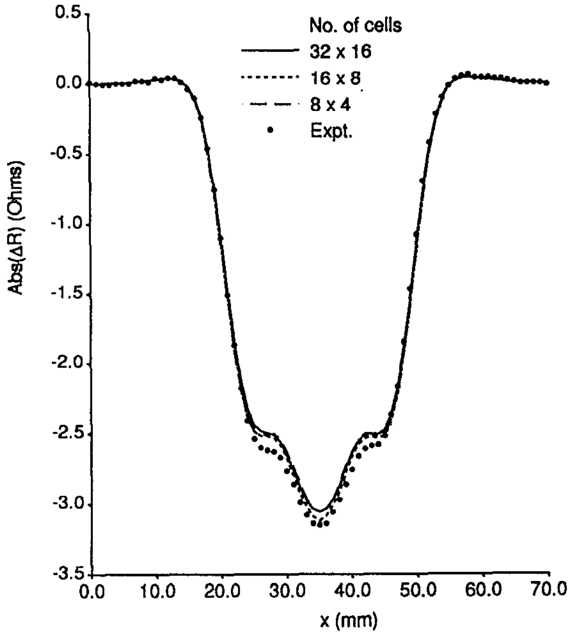

FIG. 3. Predictions of probe resistance due to a semielliptical simulated crack and comparison with experiment.

Single frequency impedance measurements were made on simulated cracks in the form of narrow slots using a normal coil. These observations were made with the coil at a number of equally spaced locations along the length of the defect. The axis of the coil was aligned with the vertical plane of the slot. Both the probe position and data collection were controlled automatically by computer. The dimensions of the coil and slots, together with other experimental parameters, are given in Table I.

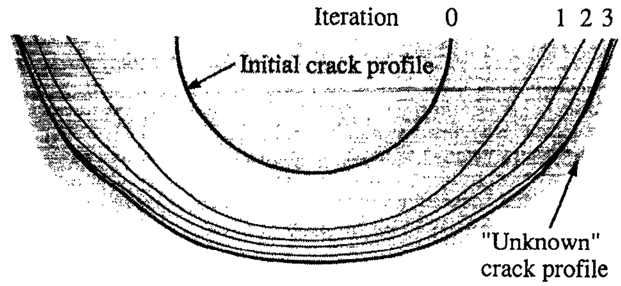

FIG. 5. Evolution of the crack profile through an iterative inversion using experimental measurements made on a semielliptical defect. The bold final crack profile was found after 15 iterations.

A discrete approximate solution of the forward problem, found using the boundary element scheme described in part I, gives the predicted probe impedance and a piecewise constant dipole density on a regular grid of rectangular elements. In order to evaluate an estimate of the impedance gradient from these results, the dipole density is sampled by interpolation at points that are at a small fixed distance from the edge of the crack. The distance being of the order of the dimensions of a boundary element. From these samples, the function $\mathscr{F}(\mathbf{m},t)$ is estimated using the half-power edge variation of the dipole density, Eq. (22). The estimates give the impedance gradient at points where vertical lines through the centers of boundary elements intersect the crack edge. The steepest descent formula is used to relocate these points and the crack profile redefined as a continuous line using a cubic spline interpolation.

Clearly there are discretization errors in this procedure, particularly as the piecewise constant approximation of the dipole density is likely to distort the dipole distribution quite

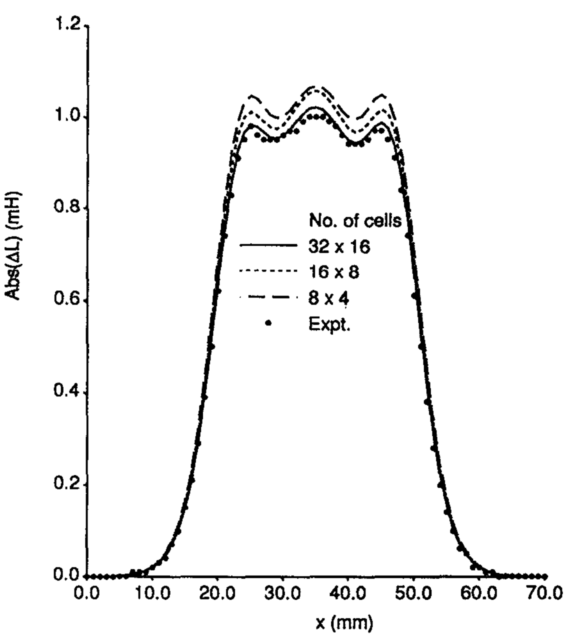

FIG. 4. Predictions of probe inductance due to a semielliptical simulated crack and comparison with experiment.

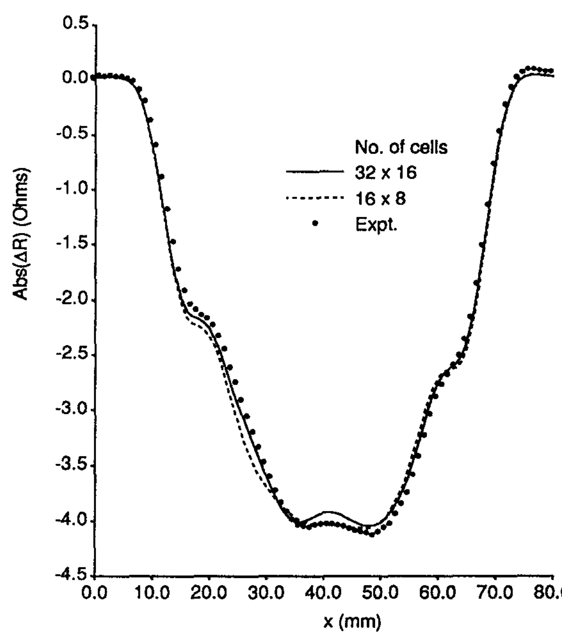

FIG. 6. Predictions of probe resistance due to an irregular simulated crack and comparison with experiment.

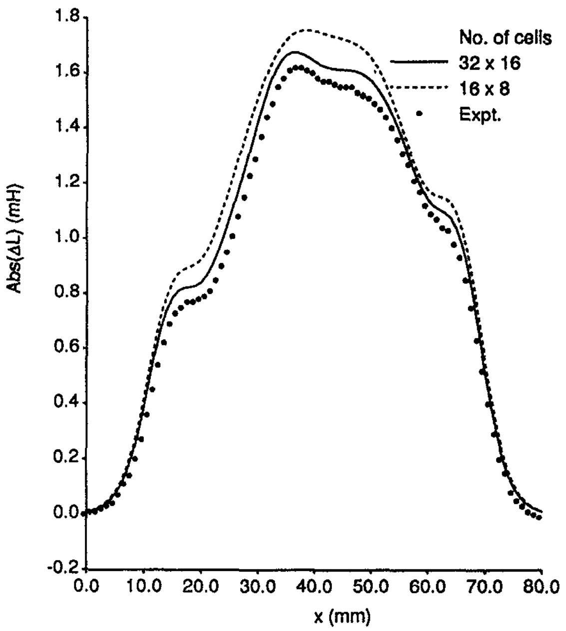

FIG. 7. Predictions of probe resistance due to an irregular simulated crack and comparison with experiment.

severely at the edge of the crack. Options for improving the accuracy of the impedance gradient calculation include increasing the number of boundary elements or reformulating the numerical scheme so that the edge behavior is enforced.[6] Both of these possibilities carry a cost penalty that needs to be constrained for the overall scheme to yield results reasonably quickly. In fact, the inversion results are reasonably accurate without the refinements.

Impedance measurements made on a slot that is nominally semielliptical are shown in Figs. 3 and 4, where they are compared with predictions calculated with three different boundary element grids. Using 51 observations, starting with a semicircular crack of radius 5 mm as the first estimate, and using a 16 boundary element grid, the inversion scheme produced the result shown in Fig. 5. In the absence of any statistical analysis of the measurements, the weight function of Eq. (5) was fixed at 1.0. After 15 iterations the global error reached 4% and thereafter did not change significantly with further processing. On completion of the calculation, the final length of the inverted crack was 21.7 mm compared with a measured value of 22.1 mm, and the depth was 8.35 mm compared with 8.61 mm measured.

It is evident from Fig. 5 that some distortion of the crack shape is produced in the regions where the edge is inclined at around 45° to the surface of the conductor. This may be due to discretization errors arising from a jagged edge approximation of the crack shape by the rectangular grid.

Observations made on an irregular simulated defect are shown in Figs. 6 and 7 where they are compared with the boundary element predictions. The inversion results using 71

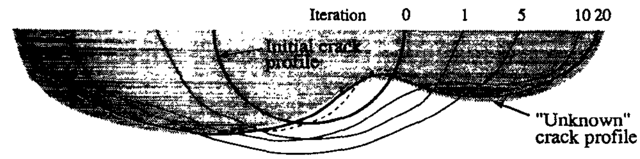

FIG. 8. Evolution of the crack profile through an iterative inversion using experimental measurements made on an irregular defect. The profile after 20 iterations is shown as a dashed line and the 100th iteration is shown bold.

observations are shown in Fig. 8. Again the initial or seed crack was semicircular, with a 5 mm radius. The boundary element grid for the inversion consisted of 32×16 cells. After 100 iterations, the calculation was terminated with crack profile that was in good agreement with the measure shape. The final calculated flaw length was 48.9 mm, compared with a measured value of 49.78 mm. The maximum depth found by inversion was 8.95 mm compared with a measured value of 8.94 mm.

VIII. CONCLUSION

An inversion scheme has been developed to reconstruct the geometry of cracks using probe impedance measurements. Tests of the inversion using observations on simulated cracks of known dimension show that the shapes can be reconstructed in reasonable time even with quite modest computer resources. All the results presented in this article could be calculated in less than 2 h on a personal computer.

Flaw inversion by optimization contains two central requirements: an effective means of predicting the observations and an efficient method of finding the gradient of the predictions with respect to a variation of the flaw. Although a boundary element scheme has been used in the present study to make the predictions, any suitable forward problem solver could be used instead. Similarly, the impedance gradient is determined by the behavior of the dipole density at the edge of the crack, therefore any numerical scheme that can be used to calculate the jump in the field or the dipole density at an ideal crack surface can be used to calculate the impedance gradient. It is not necessary to use a calculation based on an integral formulation.

ACKNOWLEDGMENT

The work of two of the authors (D. J. H. and J. R. B.) was supported by Defence Research Agency, Farnborough, and The Procurement Executive, MoD, U.K.

[1] S. J. Norton and J. R. Bowler, J. Appl. Phys. **73**, 501 (1993).
[2] J. R. Bowler, J. Appl. Phys. **75**, 8128 (1994).
[3] M. McIver, Proc. R. Soc. London Ser. **421**, 179 (1989).
[4] M. P. Connolly, D. H. Michael, and R. Collins, J. Appl. Phys. **45**, 2638 (1988).
[5] J. Hadamard, *Lectures on Cauchys's Problem in Linear Partial Differential Equations* (Dover, New York, 1952).
[6] R. DeSmelt and J. VanBladel, IEEE Trans. Antennas Propagation **AP-28**, 703 (1980).